



<b>Title</b>	Generalization of the boundary diffraction method for volume gratings
<b>Authors(s)</b>	Sheridan, John T.
<b>Publication date</b>	1994-02-01
<b>Publication information</b>	Sheridan, John T. "Generalization of the Boundary Diffraction Method for Volume Gratings." Optical Society of America, February 1, 1994. <a href="https://doi.org/10.1364/JOSAA.11.000649">https://doi.org/10.1364/JOSAA.11.000649</a> .
<b>Publisher</b>	Optical Society of America
<b>Item record/more information</b>	<a href="http://hdl.handle.net/10197/3462">http://hdl.handle.net/10197/3462</a>
<b>Publisher's statement</b>	<p>This paper was published in JOSA A: OPTICS, IMAGE SCIENCE, AND VISION and is made available as an electronic reprint with the permission of OSA. The paper can be found at the following URL on the OSA website:</p> <p><a href="http://www.opticsinfobase.org/josaa/abstract.cfm?uri=josaa-11-2-649">http://www.opticsinfobase.org/josaa/abstract.cfm?uri=josaa-11-2-649</a>. Systematic or multiple reproduction or distribution to multiple locations via electronic or other means is prohibited and is subject to penalties under law.</p>
<b>Publisher's version (DOI)</b>	10.1364/JOSAA.11.000649

Downloaded 2025-12-04 23:02:21

The UCD community has made this article openly available. Please share how this access benefits you. Your story matters! (@ucd\_oa)



© Some rights reserved. For more information

# Generalization of the boundary diffraction method for volume gratings

J. T. Sheridan

*Physikalisches Institut der Universität Erlangen-Nürnberg Staudtstrasse 7, D-8520 Erlangen, Germany*

Received January 26, 1993; revised manuscript received June 4, 1993; accepted July 20, 1993

The boundary diffraction method (BDM) is an approximate method that permits the derivation of analytic solutions for the output beams, both forward and backward propagating, that arise from the fundamental nature of holographic gratings. The method is based on the assumption that the volume scatter inside the grating can be supplemented by boundary diffraction coefficients. The boundary diffraction method is used for analysis of thick transmission geometry gratings in a unified way that deals with both the slanted and the unslanted cases. During the analysis, evidence emerges for the superiority of the first-order two-wave beta-value method over the Kogelnik  $\mathbf{k}$ -vector closure method. The BDM is then further generalized to the case of a volume transmission grating, index matched to its surroundings, and replayed normally on-Bragg, i.e., satisfying the Bragg condition for normal incidence. The analytic equations derived are compared with results calculated with the rigorous coupled-wave method.

## 1. INTRODUCTION

The boundary diffraction method<sup>1-3</sup> (BDM) can be used for deriving analytic formulas for the spurious orders that are not predicted by the usual two-wave first-order coupled-wave methods, for example the Kogelnik  $\mathbf{k}$ -vector closure method<sup>4</sup> (KVCM) and the beta-value method<sup>5</sup> (BVM). The sizes of such small spurious orders are of interest in the design of some holographical optical elements, i.e., head-up displays.<sup>6</sup> In this method the multiple scatter inside the volume grating is supplemented by boundary scatter coefficients in a manner analogous to that used in the geometrical theory of diffraction.<sup>7</sup> The BDM has been applied to unslanted transmission gratings,<sup>1</sup> slanted transmission gratings,<sup>2</sup> and symmetric reflection gratings.<sup>3</sup> The gratings are assumed perfectly index matched to their surroundings and are replayed on-Bragg, so this case differs fundamentally from analyses in which Fresnel reflections are included.<sup>8</sup>

In this paper a single formalism for dealing with slanted and unslanted transmission gratings is derived. It allows for the fact that the boundary diffracted waves may replay the grating slightly off-Bragg, i.e., slightly deviating from the Bragg condition. Analytic formulas are presented and compared with results that are produced with the rigorous coupled-wave method<sup>9</sup> (RCWM). One interesting result of this work is to provide further evidence of the superiority of the BVM over the KVCM in the prediction of the far off-Bragg response of a volume grating.<sup>10</sup> A case of particular interest, in which a transmission grating is replayed normally on-Bragg, is examined. Such a grating can be used as a deflection element in a two-dimensional interconnection system.<sup>11</sup> Three forward- and three backward-traveling waves are retained in the analysis. Significantly, although the grating is replayed on-Bragg, the symmetric higher-order off-Bragg transmitted wave will exist and may contain appreciable power. Analytic formulas for the four spurious waves are presented and are compared with those found by using the RCWM.

## 2. FULL ANALYSIS OF THE TWO-WAVE-TRANSMISSION CASE

The notation used in this paper is that which has appeared previously.<sup>2</sup> The amplitude of  $i$ th reflection order outside the grating is denoted  $R_i$ , and the  $i$ th transmitted orders are denoted  $T_i$  ( $i = +1, 0, \text{ or } -1$ ). The normalized intensities of the diffraction orders are denoted  $I_{i/z}$ , where  $z$  denotes the grating boundary from which the beam originates ( $z = 0$  or  $z = d$ ). The notation is illustrated in Fig. 1, where  $\mathbf{K}$  is the grating vector.

This section follows naturally from Refs. 1 and 2. In Ref. 1 all the propagating beams replay the volume grating on-Bragg. In Ref. 2 the boundary waves replay the volume far off-Bragg. In this section equations are derived that include the above special cases and also the case in which the boundary beams replay the volume slightly off-Bragg. Emphasis is placed on a thorough mathematical analysis, since the physical arguments have previously been discussed in some detail in the literature.

We start with the Helmholtz scalar-wave equation for TE-polarized light<sup>12</sup>:

$$\nabla^2 E_y(x, z) + \beta^2 [\epsilon_2 + \epsilon_{21} \cos(\mathbf{K} \cdot \mathbf{r})] E_y(x, z) = 0, \quad (1)$$

where the grating contains a simple cosinusoidal permittivity modulation of size  $\epsilon_{21}$ . The average permittivity of the grating  $\epsilon_2$  is assumed matched to the permittivities on either side,  $\epsilon_1 = \epsilon_2 = \epsilon_3 = 1$ . The grating has a period of size  $\Lambda$  and a grating vector of size  $K = 2\pi/\Lambda$ .  $\beta = 2\pi/\lambda$ , where  $\lambda$  is the free-space incident wavelength.

For a set of coupled-wave equations to be produced, an  $\mathbf{E}$ -field expansion in terms of the waves that exist inside the grating must be substituted into Eq. (1). The expansion has the form

$$\begin{aligned} E_y(x, z) = & A_0(z) \exp(-j\mathbf{p}_0 \cdot \mathbf{r}) + A_{+1}(z) \exp(-j\mathbf{p}_{+1} \cdot \mathbf{r}) \\ & + a_0(z) \exp[-j\boldsymbol{\sigma}_0 \cdot (\mathbf{r} - d\mathbf{i}_z)] \\ & + a_{+1}(z) \exp[-j\boldsymbol{\sigma}_{+1} \cdot (\mathbf{r} - d\mathbf{i}_z)]. \end{aligned} \quad (2)$$

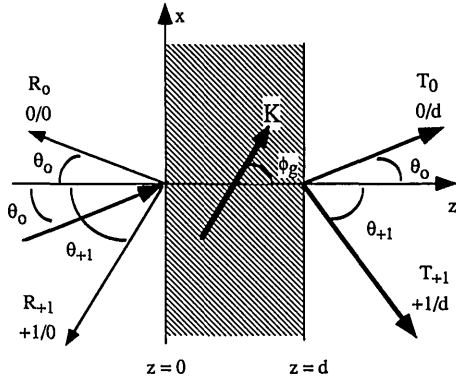


Fig. 1. Two-wave asymmetric transmission geometry grating. The volume grating is index matched to the surrounding material and has an average index of  $\epsilon_2 = 1$ .

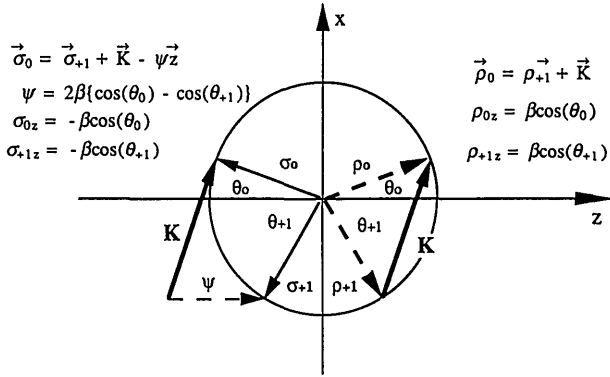


Fig. 2. Ewald diagram, BVM representation, for the asymmetric transmission case.

$A_0$  and  $A_{+1}$  are the primary forward-traveling wave amplitudes, and  $a_0$  and  $a_{+1}$  are the spurious backward-traveling wave amplitudes.  $\rho_0$ ,  $\rho_{+1}$ ,  $\sigma_0$ , and  $\sigma_{+1}$  are the corresponding wave vectors and are shown on the Ewald diagram in Fig. 2.  $\mathbf{r} - \mathbf{d}$  appears in the exponential of the  $a_i$ 's as these waves originate at the  $z = d$  grating boundary. All higher orders are neglected.

Substituting Eq. (2) into Eq. (1), eliminating all second derivatives, and expanding produce the following set of beta-value coupled-wave equations:

$$\cos(\theta_0) \frac{dA_0}{dz} + j\kappa A_{+1} = 0,$$

$$\cos(\theta_{+1}) \frac{dA_{+1}}{dz} + j\kappa A_0 = 0, \quad (3)$$

$$-\cos(\theta_0) \frac{da_0}{dz} + j\kappa a_{+1} \exp[-j(\psi z - K_z d)] = 0, \quad (4)$$

$$-\cos(\theta_{+1}) \frac{da_{+1}}{dz} + j\kappa a_0 \exp[+j(\psi z - K_z d)] = 0. \quad (5)$$

The grating coupling constant is defined as  $\kappa = \pi \epsilon_{21} / 2\lambda(\epsilon_2)^{1/2}$ , and  $\theta_0$  and  $\theta_{+1}$  are the angles of the input and the diffracted beams. The dephasing parameter is simply related to the  $z$  component of the grating vector  $\psi = 2K_z$ .

The solutions for  $A_0$  and  $A_{+1}$ , given a single input, are well known.<sup>4</sup> The solutions for  $a_0$  and  $a_{+1}$  must, however, be solved for two simultaneous input beams, the two spu-

rious waves arising at the  $z = d$  boundary. Before this analysis is carried out, the electromagnetic boundary conditions must be examined. First the tangential components of the  $\mathbf{E}$  and the  $\mathbf{H}$  fields are phase matched at  $z = 0$ . This is represented in Fig. 3.

Matching the tangential  $\mathbf{E}$  field gives that

$$1 + R_0 = A_0(0) + a_0(0) \exp(+j\sigma_0 d), \quad (6)$$

$$R_{+1} = A_{+1}(0) + a_{+1}(0) \exp(+j\sigma_{+1} d). \quad (7)$$

Matching the tangential  $\mathbf{H}$  field gives that

$$-j\rho_0(R_0 - 1) = \left[ -j\rho_0 A_0(0) + \frac{dA_0}{dz} \right]_{z=0} + \left[ -j\sigma_0 a_0(0) + \frac{da_0}{dz} \right]_{z=0} \exp(+j\sigma_0 d), \quad (8)$$

$$+j\rho_{+1} R_{+1} = \left[ -j\rho_{+1} A_{+1}(0) + \frac{dA_{+1}}{dz} \right]_{z=0} + \left[ -j\sigma_{+1} a_{+1}(0) + \frac{da_{+1}}{dz} \right]_{z=0} \exp(+j\sigma_{+1} d). \quad (9)$$

In this analysis it is assumed that  $(\epsilon_{21})^n = 0$  if  $n > 1$ . From Eqs. (3) we see that, for the primary waves,

$$\frac{dA_n(z)}{dz} \bigg|_{z=\zeta} = -j \frac{\kappa}{\cos(\theta_n)} A_m(\zeta) \quad (10a)$$

(where  $n = 0, 1$  implies that  $m = 1, 0$ ). From Eqs. (4) and (5) we see that

$$a_i(z) \propto \epsilon_{21}(i = 1, 2) \Rightarrow \frac{da_i}{dz} \propto \epsilon_{21}^2 \approx 0. \quad (10b)$$

Combining Eqs. (6), (8), and (10) gives that

$$A_{+1}(0) \propto \epsilon_{21} \Rightarrow R_0 \approx -a_0(0) \exp(+j\sigma_0 d). \quad (11)$$

Combining Eqs. (7) and (9) and relations (10) gives that

$$R_{+1} = a_{+1}(0) \exp(+j\sigma_{+1} d) - \frac{\kappa}{2 \cos(\theta_{+1}) \rho_{+1}} A_0(0), \quad (12)$$

where  $A_0(0) = 1 - O(\epsilon_{21})$ , implying that in Eq. (12)  $\kappa A_0(0) \approx \kappa$ .

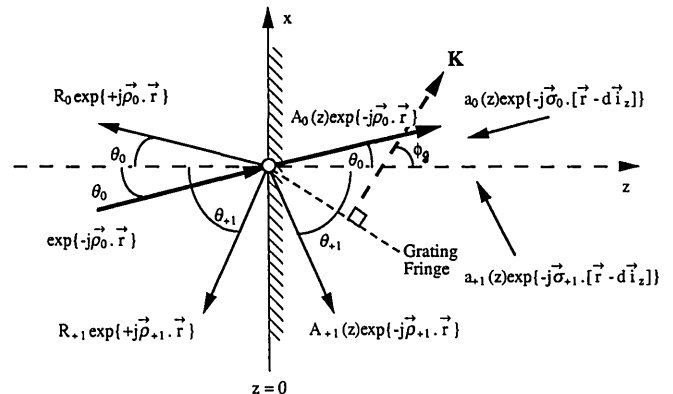


Fig. 3.  $z = 0$  boundary. All the primary and spurious waves that are incident are shown. The wave vectors of the beams and the grating vector  $\mathbf{K}$  are also shown.

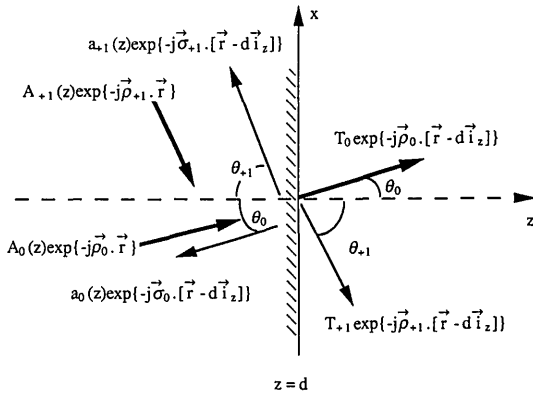


Fig. 4.  $z = d$  boundary; other information as in Fig. 3.

Thus in relations (11) and (12) we have first-order expressions for  $R_0$  and  $R_{+1}$  in terms of the waves traveling through the volume grating from the  $z = d$  boundary.

The  $z = d$  boundary is shown in Fig. 4. The same phase-matching procedure as above is followed. After the transmitted  $T_i$  beams have been eliminated, the following expressions are found:

$$\begin{aligned} a_0(d) &= \frac{\kappa}{2 \cos(\theta_0) \rho_{0z}} A_{+1}(d) \exp(-j \rho_{0z} d) \\ &= \frac{\varepsilon_{21}}{8 \cos^2(\theta_0)} j \sin(\nu) \exp[-j \beta \cos(\theta_0) d], \end{aligned} \quad (13)$$

$$\begin{aligned} a_{+1}(d) &= \frac{\kappa}{2 \cos(\theta_{+1}) \rho_{+1z}} A_0(d) \exp(-j \rho_{+1z} d) \\ &= \frac{\varepsilon_{21}}{8 \cos^2(\theta_{+1})} \cos(\nu) \exp[-j \beta \cos(\theta_{+1}) d], \end{aligned} \quad (14)$$

where  $\nu = \kappa d / [\cos(\theta_0) \cos(\theta_{+1})]^{1/2}$ .

Thus all the beam amplitudes at the two boundaries are defined in terms of the four wave amplitudes at those boundaries. These equations contain all the phase information for the beams. It is now possible to derive the analytic solutions of Eqs. (4) and (5) with two simultaneous inputs, Eqs. (13) and (14). Equations (4) and (5) are first transformed into constant coefficient differential equations by substitution of the variables

$$\begin{aligned} S_0(z) &= a_0(z) \exp[+j(\psi z - K_z d)/2] : \\ S_{+1}(z) &= a_{+1}(z) \exp[-j(\psi z - K_z d)/2]. \end{aligned} \quad (15)$$

The solutions for the two-beams output from the volume are

$$\begin{aligned} S_0(z) &= \frac{1}{2\Phi \cos(\theta_0)} \left\{ \left[ \cos(\theta_0) \left( \Phi + \frac{\psi}{2} \right) S_0(d) + \kappa S_{+1}(d) \right] \right. \\ &\quad \times \exp[+j\Phi(z - d)] \\ &\quad - \left[ \kappa S_{+1}(d) - \cos(\theta_0) \left( \Phi - \frac{\psi}{2} \right) S_0(d) \right] \\ &\quad \times \exp[-j\Phi(z - d)] \Big\}, \end{aligned} \quad (16)$$

$$\begin{aligned} S_{+1}(z) &= \frac{1}{2\Phi \kappa} \left\{ \left( \Phi - \frac{\psi}{2} \right) \right. \\ &\quad \times \left[ \cos(\theta_0) \left( \Phi + \frac{\psi}{2} \right) S_0(d) + \kappa S_{+1}(d) \right] \\ &\quad \times \exp[+j\Phi(z - d)] - \left( \Phi + \frac{\psi}{2} \right) \\ &\quad \times \left[ \kappa S_{+1}(d) - \cos(\theta_0) \left( \Phi - \frac{\psi}{2} \right) S_0(d) \right] \\ &\quad \times \exp[-j\Phi(z - d)] \Big\}, \end{aligned} \quad (17)$$

where  $\Phi = [\nu^2 + (\psi/2)^2]^{1/2}$ .

The relationships between the  $S_i$ 's and the  $a_i$ 's at  $z = d$  and  $z = 0$  are given by Eqs. (15). Thus the  $a_i$ 's are fully defined at both boundaries. It is now possible for us to return to relation (11) to calculate  $R_0$  or to Eq. (12) to calculate  $R_{+1}$ .

This result can be tested in comparison with the analytic expressions for the symmetric<sup>1</sup> and the very asymmetric<sup>2</sup> transmission geometry cases. For the second case, for far off-Bragg replay by the boundary scatter, the following limit can be used on Eqs. (16) and (17):

$$\psi \gg \nu \Rightarrow \Phi \approx \psi/2 = K_z. \quad (18)$$

The volume has no effect on an input beam; therefore  $a_0(0) = a_0(d)$  and  $a_{+1}(0) = a_{+1}(d)$ . Substitution of the above equations into relations (11) and (12) for the  $R_0$  and  $R_{+1}$  beams reproduces Eqs. (32) and (33) of Ref. 2. Similar agreement is found with Eq. (3) of Ref. 1 when  $\psi = 0$ .

### 3. RESULTS FOR THE FULL TWO-WAVE CASE

The expressions derived in Section 2 are compared with results calculated by the RCWM.<sup>9</sup> We examine the case when  $\varepsilon_{21}/\varepsilon_2 = 1/20$ . The breakdown of the BDM has been associated with two effects.<sup>1-3</sup> First, the boundary diffraction coefficient may become inaccurate. This will occur either in the case of large permittivity modulation or when the diffraction angle becomes large. Second, breakdown occurs if the angle of diffraction becomes small and the field in the grating is not well approximated by a two-wave expansion.

A second question is also tackled here. The BDM expressions presented in Section 2 were derived with the BVM.<sup>5</sup> It has been found that in the case of an unslanted transmission grating<sup>10</sup> the results for off-Bragg incidence from the BVM differ from the results from Kogelnik's KVCM.<sup>4</sup> This difference was examined, and the BVM was found to be superior. A set of BDM equations analogous to Eqs. (16) and (17) can be derived starting with the KVCM form of Eqs. (4) and (5). The effectiveness of the two different sets of BDM equations for slanted transmission gratings is examined.

In Fig. 5(a) and 5(b),  $I_{0/0}$ (BVM) and  $I_{0/0}$ (KVCM), respectively, are plotted as functions of grating thickness, and the results are compared with the unique RCWM result. The grating examined is recorded with beams incident at 30° and 26°, which creates a grating with a grating slant angle of  $\phi_g = 92^\circ$ . The grating is replayed at 30°, as is

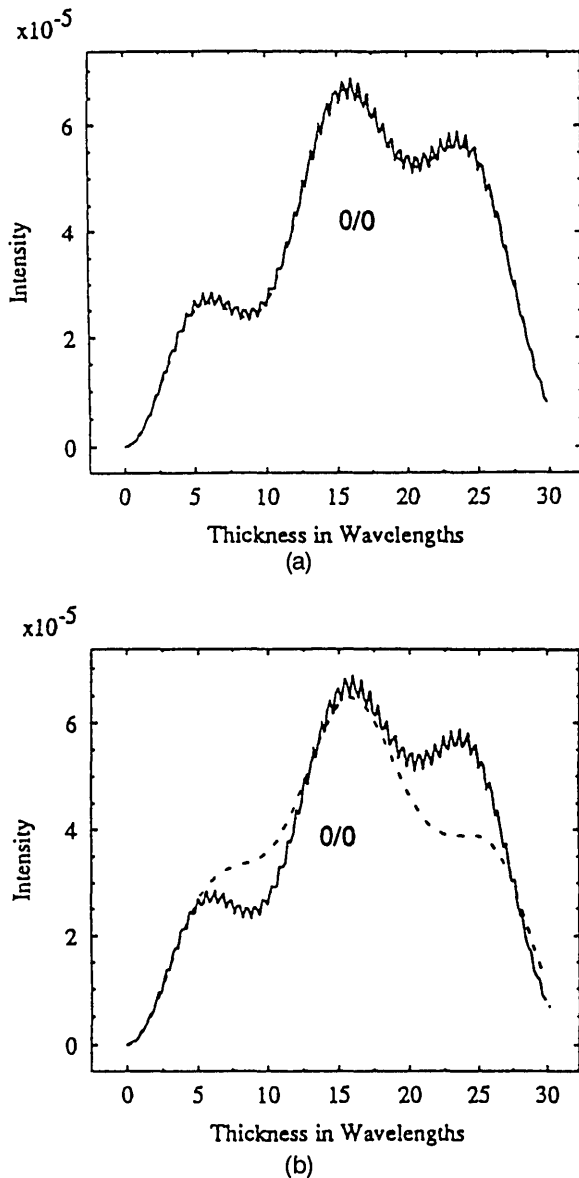


Fig. 5. (a) Comparison of the BDM-BVM result (dashed curve) with the RCWM result (solid curve) for the spurious reflection order,  $I_{00}$ , with  $\theta_1 = 30^\circ$ ,  $\theta_2 = 26^\circ$ , and  $\phi_g = 92^\circ$ . Normalized diffraction efficiency as a function of the grating thickness is shown. (b) The BDM-KVCM result (dashed curve) is compared with the RCWM result (solid curve) for the same grating as in (a). The agreement is not so good as in (a).

illustrated in Fig. 6. From Fig. 5 it can be seen that (1) the BVM results agree more closely with the RCWM results than with the KVCM results, and (2) the agreement of the BDM that is based on the BVM is good. We also examined the case in which  $\phi_g = 85^\circ$  and the spurious beams replay the grating further off-Bragg. In this case the difference between the two sets of analytic equations decreased, but the BVM-based BDM is still better. When the grating is unslanted,  $\phi_g = 90^\circ$ , the two sets of BDM equations are identical, as shown in Ref. 1.

The BDM as described so far differentiates clearly between the volume and the boundary effects; however, the boundary coefficients do contain information regarding the geometry of the volume grating. The inclusion of obliquity factors in the analysis is very important, since

the factors clearly distinguish between the power traveling in the  $z$  direction and the wave amplitudes.

#### 4. THREE-WAVE TRANSMISSION CASE

The case to be discussed here is illustrated in Fig. 7, and the corresponding Ewald diagram is shown in Fig. 8. It is

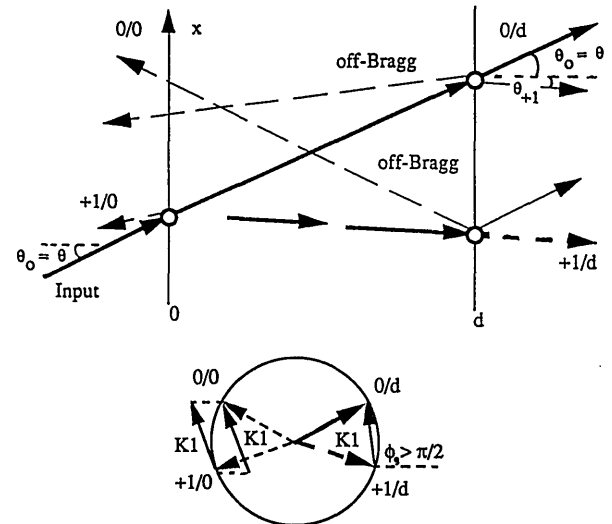


Fig. 6. Transmission grating,  $\phi_g > 90^\circ$ , and its Ewald diagram. Thick lines, primary beams; thin dashed lines, spurious boundary diffracted waves. This is the case examined in Fig. 5.

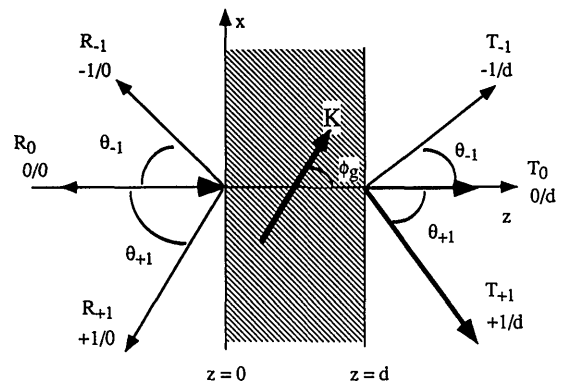


Fig. 7. Three-wave transmission case. The grating is index matched to its surroundings, and the input beam is incident normally on-Bragg.

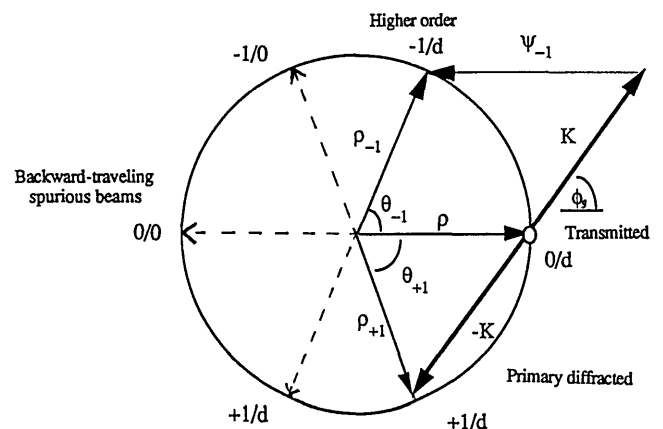


Fig. 8. Ewald diagram for Fig. 7. All six BVM wave vectors are shown. The  $-1/d$  forward order is produced by off-Bragg replay of the volume grating.  $\theta_{+1} = \theta_{-1} = \theta$ .

assumed that the grating operates in the thick regime,  $\Omega > 20$ .<sup>13</sup> Despite the strong Bragg effect, six waves travel outside the volume grating. The particularly significant fact in this case is that one of the forward-traveling waves is produced in part by off-Bragg replay of the volume grating. Therefore boundary diffraction coefficients arise as a result of off-Bragg replay.

### A. Mathematical Analysis

The following BVM coupled-wave equations are found for the transmitted beams:

$$\frac{d^2 A_{-1}(z)}{dz^2} - 2j\beta \cos(\theta) \frac{dA_{-1}(z)}{dz} + 2\beta\kappa A_0(z) \exp(-j\psi_{-1}z) = 0, \quad (19a)$$

$$\frac{dA_0(z)}{dz} + j\kappa[A_{+1}(z) + A_{-1}(z) \exp(+j\psi_{-1}z)] = 0, \quad (19b)$$

$$\cos(\theta) \frac{dA_{+1}(z)}{dz} + j\kappa A_0(z) = 0. \quad (19c)$$

The second derivatives of the primary waves  $A_0$  and  $A_{+1}$  are assumed negligible, and their dephasing parameters are zero.

The off-Bragg  $A_{-1}$  beam's dephasing parameter is

$$\psi_{-1} = 2\beta[1 - \cos(\theta_{-1})], \quad \nu = \frac{\kappa}{\sqrt{\cos(\theta_{+1})}}.$$

$\nu$ , as defined here, does not contain the grating thickness  $d$ . The angles of the +1st and -1st diffraction orders are equal,  $\theta_{-1} = \theta_{+1} = \theta$ . The second derivative of the  $A_{-1}$  harmonic cannot be neglected, as it is produced in the grating off-Bragg and can be proportional to  $\varepsilon_{21}$ . Since  $A_{-1}$  can be proportional to  $\varepsilon_{21}$ , the  $\kappa A_{-1}$  term in Eq. (19b) can be neglected.

The phase-matched boundary conditions for the -1st order must first be examined at both  $z = 0$  and  $z = d$ . To do so one must find an expression for the spurious wave from the  $z = d$  boundary. In the following equations  $A_{-1(\text{backscatter})}$  represents the scatter from  $z = d$  that reaches  $z = 0$ .

Matching the  $\mathbf{E}$  fields  $\mathbf{E}(0^+) = \mathbf{E}(0^-)$  for the -1 order gives

$$R_{-1} = A_{-1}(0) + A_{-1(\text{backscatter})}, \quad (20)$$

and matching  $\mathbf{H}(0^+) = \mathbf{H}(0^-)$  gives

$$+j\beta \cos(\theta) R_{-1} = \left. \frac{dA_{-1}(z)}{dz} \right|_{z=0} - j\beta \cos(\theta) A_{-1}(0) + j\beta \cos(\theta) A_{-1(\text{backscatter})}. \quad (21)$$

Substituting for  $R_{-1}$  from Eq. (20) gives that

$$\left. \frac{dA_{-1}(z)}{dz} \right|_{z=0} = +j2\beta \cos(\theta) A_{-1}(0). \quad (22)$$

Combining this equation with Eq. (19a) gives

$$A_{-1}(0) = -\frac{\kappa}{2\beta \cos^2(\theta)} - \frac{1}{4\beta^2 \cos^2(\theta)} \left. \frac{d^2 A_{-1}(z)}{dz^2} \right|_{z=0}, \quad (23)$$

which shows the dependence of the off-Bragg boundary scatter on the second derivative.

Equation (19a) can now be solved for  $A_{-1}(z)$  with use of the analytic solution  $A_0(z) = A_0(0) \cos(\nu z)$ . Equation (22) is used to provide initial conditions at  $z = 0$  in terms of  $A_{-1}(0)$ .

The solution for the diffracted order is found to be

$$A_{-1}(z) = A_{-1}(0) \exp[+j2\beta \cos(\theta)z] - 2\beta\kappa \left\{ -\frac{\cos(\nu z) \exp(-j\psi_{-1}z)}{\psi_{-1}[2\beta \cos(\theta) + \psi_{-1}]} + \frac{1}{2\beta \cos(\theta) \psi_{-1}} - \frac{\exp[+j2\beta \cos(\theta)z]}{2\beta \cos(\theta)[2\beta \cos(\theta) + \psi_{-1}]} \right\}. \quad (24)$$

The  $\mathbf{E}$  field for the -1st order must also be matched at  $z = d$ :

$$T_{-1} = A_{-1}(d) \exp[-j\beta \cos(\theta)d] - A_{-1}(0) \cos(\nu d) \exp[-j\beta[2 - \cos(\theta)]d], \quad (25)$$

and the  $\mathbf{H}$  field  $\mathbf{H}(d^+) = \mathbf{H}(d^-)$ :

$$[-j\beta \cos(\theta)] A_{-1}(d) \exp[-j\beta \cos(\theta)d] + \left. \frac{dA_{-1}(z)}{dz} \right|_{z=d} \exp[-j\beta \cos(\theta)d] - [+j\beta \cos(\theta)] A_{-1}(0) \cos(\nu d) \exp[-j\beta[2 - \cos(\theta)]d] = [-j\beta \cos(\theta)] T_{-1}. \quad (26)$$

Combining Eqs. (25) and (26) produces the following expression for the first derivative at  $z = d$ :

$$\left. \frac{dA_{-1}(z)}{dz} \right|_{z=d} = [+j2\beta \cos(\theta)] A_{-1}(0) \cos(\nu d) \exp(-j\psi_{-1}d). \quad (27)$$

No expression for the boundary scatter coefficient of the -1st order has yet been derived. For this to be done the first derivative of the function derived for  $A_{-1}(z)$  in Eq. (24) is equated with the expression for the first derivative at the boundary  $z = d$  from Eq. (27). The result is that

$$A_{-1}(0) = \frac{-\kappa}{\cos(\theta)[2\beta \cos(\theta) + \psi_{-1}]} = -\frac{\varepsilon_{21}}{8 \cos(\theta)}. \quad (28)$$

Unlike the on-Bragg boundary coefficient, the scatter is found to be inversely proportional to  $\cos(\theta)$ , not  $\cos^2(\theta)$ . Unfortunately, the boundary and volume effects are not as obviously separable in this case as in the previous analyses in the literature. However, once the correct boundary coefficient and volume expressions are derived, the matrix method that is used in Ref. 2 can be applied, 6 × 6 matrices being necessary.

Substituting Eq. (28) into Eq. (24) and using Eq. (26) gives

$$T_{-1} \exp[+j\beta \cos(\theta)d] = \left\{ -\frac{\varepsilon_{21}}{8 \cos(\theta)[1 - \cos(\theta)]} \right\} [1 - \cos(\nu d) \exp(-j\psi_{-1}d)], \quad (29)$$

and the power in this beam in the +z direction is  $I_{1/d} = |T_{-1}|^2 \cos(\theta)$ .

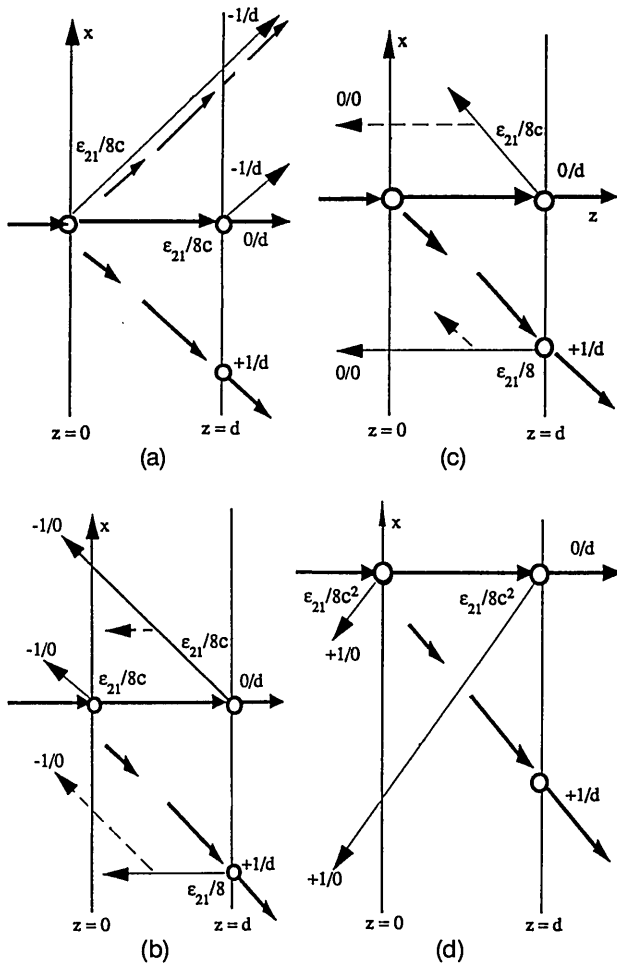


Fig. 9. (a) Three contributions to  $T_{-1}$ : the off-Bragg boundary diffraction at both boundaries and the off-Bragg volume contribution. (b) Three contributions to  $R_{-1}$ : an off-Bragg scatter from the  $z = 0$  boundary and two spurious beams resulting from scatter at the  $z = d$  boundary, one from an off-Bragg boundary scatter and the other from an on-Bragg scatter. Both of these spurious beams replay the volume grating on-Bragg. (c) Contributions to  $R_0$ . Both are due to the on-Bragg replay of the volume grating by two spurious waves, one on-Bragg boundary scatter and the other off-Bragg, arising at  $z = d$ . (d) Contributions to  $R_{+1}$ : the on-Bragg boundary scatter arising at  $z = 0$  and the on-Bragg boundary scatter arising at  $z = d$ , which replays the volume grating off-Bragg.

The waves contributing to this spurious order are represented schematically in Fig. 9(a). In this figure, thick lines are primary waves, thin lines are boundary scattered waves, and dashed lines are waves that have undergone volume diffraction. The boundary diffraction coefficients are shown where the beams arise, where  $c = \cos(\theta)$ .

The second derivative of  $A_{-1}(z)$  at  $z = 0$  is equal to

$$\left. \frac{d^2 A_{-1}(z)}{dz^2} \right|_{z=0} = -\kappa \psi_{-1}. \quad (30a)$$

If the boundary scatter is nonexistent, then

$$\left. \frac{d^2 A_{-1}(z)}{dz^2} \right|_{z=0} = -2\beta\kappa. \quad (30b)$$

In both cases the second derivative is proportional to  $\epsilon_{21}$ .

Why has the boundary contribution to this wave not been noticed previously? If the second derivative of the  $A_{-1}$  order is neglected in Eq. (19a) and the equation is solved by substituting for  $A_0(z)$  and integrating, the same equations, Eqs. (30), are found as in our analysis.

$R_0$ ,  $R_{+1}$ , and  $R_{-1}$  remain to be examined. We deal with these waves in a more phenomenological manner. In each case a figure is drawn showing the various contributions to the wave. Then, by following a simple set of rules, the relevant analytic equations for the beams can be found.

The beams scattered by the  $z = d$  boundary in the reflection direction can be defined in simple steps. The two primary-wave amplitudes arriving at  $z = d$  are

$$A_0(0)\cos(\nu d)\exp(-j\beta d), \quad (31a)$$

$$-jA_0(0)\left(\frac{c_r}{c_s}\right)^{1/2} \sin(\nu d)\exp[-j\beta \cos(\theta)d], \quad (31b)$$

where the obliquity factors are  $c_r = \cos(\theta_{in}) = 1.0$  and  $c_s = \cos(\theta)$ .

These beams are scattered. The amplitude of the scatter must be the same size as, but of opposite sign to, the corresponding scatter at the  $z = 0$  boundary (based on the fact that these beams must cancel as  $d$  goes to zero). A phase term is introduced by the relative shift of the  $z = d$  boundary grating with respect to the  $z = 0$  boundary grating. Such a situation is analogous to that which arises when two stacked volume transmission gratings are moved parallel to one another.<sup>14</sup> This has the form

$$\phi(d) = 2\pi \frac{d}{\Lambda/\cos(\phi)} = K_z d = \beta[1 - \cos(\theta)]d. \quad (32)$$

Therefore the off-Bragg boundary scatter coefficient into the volume grating from the  $z = d$  boundary combines the negative of the boundary diffraction coefficient given in Eq. (28) with the phase shift in Eq. (32). It is therefore

$$-A_{-1}(0)\exp[-j\beta[1 - \cos(\theta)]d]. \quad (33)$$

This wave is traveling in the  $-z$  direction, and so its wave-vector component in this direction is  $\beta \cos(\theta)(z - d)$ .

Using this simple methodology we can now find the expression for  $R_{-1}$ . The generation of this wave is represented in Fig. 9(b), which follows the format of Fig. 9(a). As can be seen, there are three contributions. One is from the  $z = 0$  boundary scatter, and two arise as a result of volume interactions of spurious light from the  $z = d$  boundary. The volume interactions are on-Bragg. Equation (20) governs this situation, giving that

$$R_{-1} = \frac{\epsilon_{21}}{8 \cos(\theta)} (1 + [\cos^2(\nu d) + \sin^2(\nu d)] \times \exp\{-j\beta[1 + \cos(\theta)]d + j\phi(d)\}), \quad (34)$$

and  $I_{1/0} = |R_{-1}|^2 \cos(\theta)$ .

Turning our attention to  $R_0$  and  $R_{+1}$ , we find that many of the ideas from Section 2 work well. Figures 9(c) and 9(d) illustrate the various contributions to these waves.

The analytic expression for  $R_0$  is

$$R_0 \approx \frac{\epsilon_{21}}{8} \frac{\sin(2\nu d)}{\sqrt{\cos(\theta)}}, \quad (35)$$

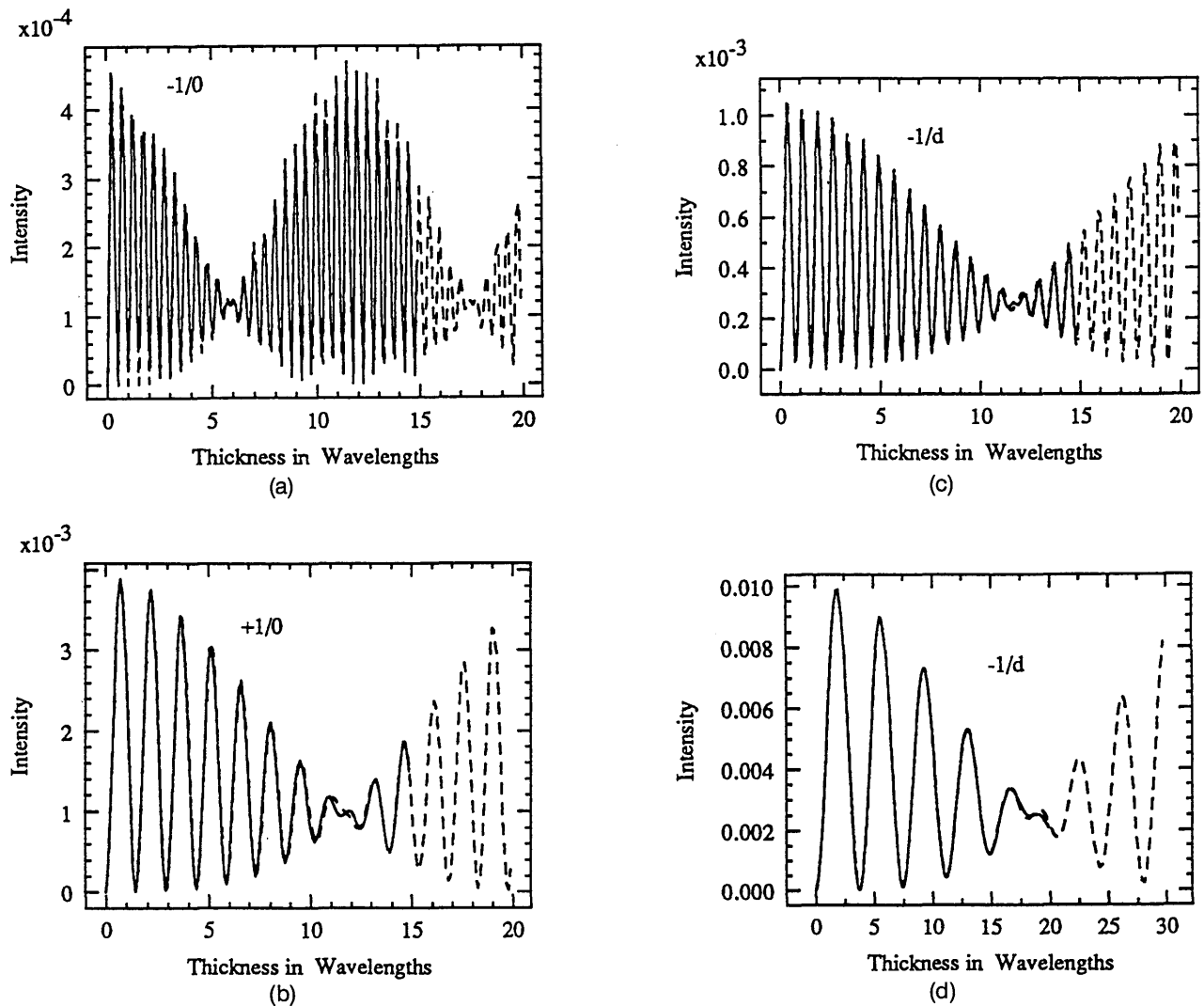


Fig. 10.  $I_{-1/0}(z)$ . The solid curve is the approximate curve from Eq. (34). The dashed curve is the RCWM curve. The slant angle  $\phi_g = 35^\circ$ ; the diffract angle is  $\theta_2 = 70^\circ$ . (b)  $I_{+1/0}(z)$ . The solid curve is the approximate curve from expression (36). Other information is as in (a). (c)  $I_{-1/d}(z)$ . The solid curve is the approximate curve from Eq. (29). Other information is as in (a). (d)  $I_{-1/d}(z)$  for a grating with  $\phi_g = 15^\circ$  and  $\theta_2 = 30^\circ$ . The solid curve is the approximate curve from Eq. (29). The dashed curve is the RCWM curve.

and  $I_{0/0} = |R_0|^2$ . For  $R_{+1}$ ,

$$R_{+1} \approx \frac{\epsilon_{21}}{8 \cos^2(\theta)} \{1 + \cos(\nu d) \exp[-j 2\beta \cos(\theta) d]\}, \quad (36)$$

and  $I_{+1/0} = |R_{+1}|^2 \cos(\theta)$ .

$A_{-1}(d)$  will be scattered at the far boundary, leading, when it is large, to strong oscillations on the other boundary scattered beams. This is an example of the breakdown that occurs because of the use of the first-order approximation.

Can any of the reflected spurious beams be equivalent in size to the forward-traveling spurious beam? One can equate the  $R_{+1}$  beam amplitude and the forward  $T_{-1}$  beam amplitudes to find the angle at which they have the same size:

$$\frac{\epsilon_{21}}{8 \cos^2(\theta)} = \frac{\epsilon_{21}}{8[1 - \cos(\theta)]\cos(\theta)} \Rightarrow \cos(\theta) = \frac{1}{2}. \quad (37)$$

Therefore if  $\theta > 60^\circ$ ,  $|R_{+1}|$ , which is frequently neglected, can be greater than  $|T_{-1}|$ .

## B. Comparison of the Analytic and the Rigorous Results

In Fig. 10, curves calculated with the RCWM and the fits to these curves calculated with analytic expressions from Subsection 4.A are compared. In the graphs the intensities of the various diffraction orders as functions of the grating thickness are plotted. In all cases  $\epsilon_{21}/\epsilon_2 = 1/20$ . The RCWM result is represented by dashed curves, and the solid curves are the corresponding approximate analytic predictions. In Figs. 10(a)–10(c) the curves are for the case of a grating whose diffraction angle is  $70^\circ$ ; i.e., the grating slant angle is  $\phi_g = 35^\circ$ . In Fig. 10(d),  $I_{-1/d}$  is plotted for a grating that has a diffraction angle of  $30^\circ$ , and therefore  $\phi_g = 15^\circ$ . In all the graphs the RCWM and BDM results agree to within a few percentage points.

## 5. CONCLUSION

The boundary diffraction method (BDM) has been generalized to deal with the full two-wave-transmission grating case. Evidence for the superiority of the first-order beta-value method (BVM) over the Kogelnik  $\mathbf{k}$ -vector closure



method (KVCN) has emerged during this analysis. The BDM is further generalized to the case of a transmission grating replayed normally on-Bragg. In this case, waves produced by off-Bragg replay of the volume grating exist. Three forward- and three backward-traveling waves are retained in the analysis, and analytic equations describing the variation of the spurious beams are derived. These compare well with the predictions of the rigorous coupled-wave method (RCWM) for the range of typical holographic parameters. The BDM has therefore been shown to remain useful as the number of orders increases.

The KVCN has been applied in the analysis of surface-relief gratings manufactured holographically in photoresist<sup>15,16</sup> and other surface-relief optical elements.<sup>17</sup> In the first case the gratings are closely index matched to their surroundings.<sup>15</sup> In the others the average index of the gratings differs considerably from the surrounding material,<sup>16,17</sup> and strong étalon effects may occur. In addition, the permittivity modulation term is large compared with the usual holographic grating. It does seem, however, that the use of the BDM might allow a better physical insight to be achieved in these cases.

## ACKNOWLEDGMENTS

The author thanks L. Solymar, D. Webb, and A. Ramsbottom of Pilkington's Plc, Lathom. The author currently holds a European Community Fellowship at the Department of Applied Optics of the University of Erlangen-Nürnberg.

## REFERENCES

1. J. T. Sheridan and L. Solymar, "Boundary diffraction coefficients for calculating spurious beams produced by volume gratings," *Electron. Lett.* **26**, 1840-1841 (1990).
2. J. T. Sheridan and L. Solymar, "Diffraction by volume gratings: approximate solution in terms of boundary diffraction coefficients," *J. Opt. Soc. Am. A* **9**, 1586-1591 (1992).
3. J. T. Sheridan and L. Solymar, "Spurious beams in reflection gratings: a solution in terms of boundary diffraction coefficients," *Opt. Commun.* **94**, 8-12 (1992).
4. H. Kogelnik, "Coupled wave theory for thick hologram gratings," *Bell Syst. Tech. J.* **48**, 2909-2945 (1969).
5. N. Uchido, "Calculation of the diffraction efficiency in hologram gratings attenuated along the direction perpendicular to the grating vector," *J. Opt. Soc. Am.* **63**, 280-387 (1973).
6. A. Ramsbottom, "Characteristics and properties of powered reflection holographic optical elements," *Optoelectronics* **5**, 606-614 (1990).
7. G. L. James, *Geometrical Theory of Diffraction for Electromagnetic Waves*, IEE Electromagnetic Wave Series (Pergamon, London, 1976).
8. M. P. Owen, A. A. Ward, and L. Solymar, "Internal reflections in bleached reflection holograms," *Appl. Opt.* **22**, 159-163 (1983).
9. T. K. Gaylord and M. G. Moharam, "Analysis and application of optical diffraction by gratings," *Proc. Inst. Electr. Eng.* **73**, 894-937 (1985).
10. J. T. Sheridan, "A comparison of diffraction theories for off-Bragg replay," *J. Mod. Opt.* **39**, 1709-1718 (1992).
11. H. Kobolla, J. T. Sheridan, E. Gluch, J. Schmidt, R. Voelkel, J. Schwider, and N. Streibl, "Holographic 2-D mixed polarization deflection elements," *J. Mod. Opt.* **40**, 613-624 (1993).
12. L. Solymar and D. J. Cooke, *Volume Holography and Volume Gratings* (Academic, London, 1981).
13. R. R. A. Syms, *Practical Volume Holography* (Clarendon, Oxford, 1990).
14. J. T. Sheridan, "Stacked volume holographic gratings. Part I: transmission gratings in series," *Optik* (to be published).
15. H. J. Gerritsen, "Dispersion effects in relief holograms immersed in near index matched liquids or Christiansen revisited," *Appl. Opt.* **25**, 2382-2385 (1986).
16. H. J. Gerritsen, D. K. Thornton, and S. R. Bolton, "Application of Kogelnik's two-wave theory to deep, slanted, highly efficient, relief transmission gratings," *Appl. Opt.* **30**, 807-814 (1991).
17. J. Maser and G. Schmal, "Coupled wave description of the diffraction by zone plates with high aspect ratios," *Opt. Commun.* **89**, 355-362 (1992).